AMERICAN SOCIETY FOR MICROBIOLOGY | Journal of Bacteriology

The Last *r* Locus Unveiled: T4 RIII Is a Cytoplasmic Antiholin

Yi Chen,[a,b] Ry Young[a,b]

Department of Biochemistry and Biophysics, Texas A&M University, College Station, Texas, USA[a]; Center for Phage Technology, Texas A&M University, College Station, Texas, USA[b]

ABSTRACT

The latent period of phage T4, normally ~25 min, can be extended indefinitely if the infected cell is superinfected after 5 min. This phenomenon, designated lysis inhibition (LIN), was first described in the 1940s and is genetically defined by mutations in diverse T4 *r* genes. RI, the main effector of LIN, has been shown to be secreted to the periplasm, where, upon activation by superinfection with a T-even virion, it binds to the C-terminal periplasmic domain of the T4 holin T and blocks its lethal permeabilization of the cytoplasmic membrane. Another *r* locus, *rIII*, has been the subject of conflicting reports. In this study, we show that RIII, an 82-amino-acid protein, is also required for LIN in both *Escherichia coli* B strains and *E. coli* K-12 strains. In T4Δ*rIII* infections, LIN was briefly established but was unstable. The overexpression of a cloned *rIII* gene alone impeded T-mediated lysis temporarily. However, coexpression of *rIII* and *rI* resulted in a stable LIN state. Bacterial two-hybrid assays and pulldown assays showed that RIII interacts with the cytoplasmic N terminus of T, which is a critical domain for holin function. We conclude that RIII is a T4 antiholin that blocks membrane hole formation by interacting directly with the holin. Accordingly, we propose an augmented model for T4 LIN that involves the stabilization of a complex of three proteins in two compartments of the cell: RI interacting with the C terminus of T in the periplasm and RIII interacting with the N terminus of T in the cytoplasm.

IMPORTANCE

Lysis inhibition is a unique feature of phage T4 in response to environmental conditions, effected by the antiholin RI, which binds to the periplasmic domain of the T holin and blocks its hole-forming function. Here we report that the T4 gene *rIII* encodes a cytoplasmic antiholin that, together with the main antiholin, RI, inhibits holin T by forming a complex of three proteins spanning two cell compartments.

The *r* genes of the T-even phages, first identified by laboratories of the Phage Group in the 1940s (1, 2), have a special place in the history of molecular biology. Detailed studies of the first three loci discovered—*rI*, *rIIAB*, and *rIII*—were foundational in working out the fundamentals of inheritance, genetic code, mutation, recombination, DNA repair, and gene structure (3–7). These mutable loci were originally discovered by their distinctive plaque morphology: large, clear, sharply defined plaques, easily distinguished from the small, fuzzy-edged, turbid plaques of the parental phages (1). The "*r*" designation meant "rapid lysis," which refers to the observation that the mutant phages isolated from the r-type plaques caused rapid, culture-wide lysis at ~25 min after infection, whereas cultures infected with the parental phages continued to increase in mass and accumulate progeny virions intracellularly for hours, in a state called "lysis inhibition"(LIN) (8). In the ensuing decades, more loci were classified as *r* genes based on mutant plaque phenotypes; at one point, *r* genes numbering up to *rVI* were assigned map positions (9, 10). In 1998, Paddison et al. (11) reviewed this field and concluded that only *rI*, *rIII*, and *rV* were directly involved in LIN, while the other genes caused lysis phenotypes through indirect physiological pathways. The *rV* mutants were shown to be missense alleles of gene *t*, which encodes T, the holin of phage T4 (12). Holins are the master lysis control proteins of the *Caudovirales* (13), acting to terminate the infection cycle by permeabilizing the cytoplasmic or inner membrane (IM) at a programmed time. It followed that the simplest operational model to explain the involvement of the remaining loci associated with direct LIN defects, *rI* and *rIII*, would be that the RI and RIII proteins were required to inhibit the lethal function of T and thus establish the LIN state (9, 11).

More-recent studies on T and RI have confirmed aspects of this operational model for LIN and provided molecular details for the lysis pathway of T4 (14–16). Like other holins, including the well-studied S105 holin of phage lambda, the T holin accumulates harmlessly in the host IM until it suddenly forms lethal, micrometer-scale membrane lesions at an allele-specific time. This event, which is defined as holin triggering, results in the escape of the cytoplasmic endolysin E (the product of gene *e*) (13) into the periplasm, where it rapidly degrades the cell wall. In turn, the loss of cell wall activates the spanin complex (the product of *pseT.2* and *pseT.3*) (17), which then disrupts the outer membrane (OM) and completes the release of the progeny. In single infections, T4 completes this three-step pathway in ~25 min (1). However, if the T4-infected cells are superinfected by other T4 (or T-even phages) after the first 5 min of the infection cycle, LIN is imposed (18). There has been progress on the molecular basis of LIN (15, 19–21). While most holins have two or more transmembrane domains (TMDs) and only short soluble loops connecting them (13), the T holin has a unique structure, with only a single TMD and significant N-terminal (34-amino-acid [34-aa]) and C-termi-

Received 8 April 2016 **Accepted** 27 June 2016

Accepted manuscript posted online 5 July 2016

Citation Chen Y, Young R. 2016. The last *r* locus unveiled: T4 RIII is a cytoplasmic antiholin. J Bacteriol 198:2448–2457. doi:10.1128/JB.00294-16.

Editor: P. J. Christie, McGovern Medical School

Address correspondence to Ry Young, ryland@tamu.edu.

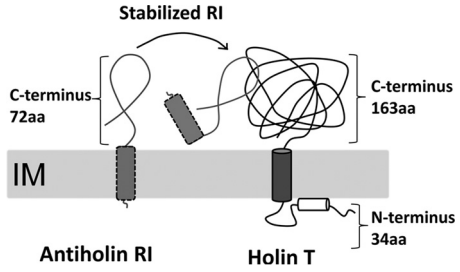

FIG 1 Topology of T4 holin T-antiholin RI interaction. T is an inner membrane protein with a single TMD (shown as a filled cylinder) and an amphipathic helix (shown as an open cylinder). RI has a SAR (signal anchor release) domain (shown as a rectangle with a dashed outline) that allows RI to be released spontaneously into the periplasm (19). If stabilized by the LIN signal, periplasmic RI binds to the C-terminal globular periplasmic domain of T. IM, inner membrane.

nal (163-aa) cytoplasmic and periplasmic domains, respectively (15, 22) (Fig. 1). Moreover, the RI protein has been shown to have a SAR (*s*ignal *a*nchor *r*elease) domain, which is a TMD that can escape from the membrane (19). By virtue of this domain, RI is secreted initially as a membrane-tethered periplasmic protein and is then released into the periplasm, where, in single infections, it is degraded rapidly (19, 20). However, under LIN conditions (i.e., when there is superinfection with a second T4 phage particle), RI is stabilized and accumulates in the periplasm, where it forms an equimolar complex with the cytoplasmic domain of T and inhibits triggering, thus imposing the LIN state. Additionally, if the SAR domain of RI is replaced by cleavable signal peptidase I, the processed RI protein overaccumulates in the periplasm in a stable, mature form, forms the complex with T, and imposes LIN without requiring activation by superinfection (19, 20).

Because RI is a specific inhibitor of T, it is formally a member of a diverse class of proteins designated antiholins (23–26). Moreover, since RI inhibits T only under certain physiological conditions, it is the only antiholin known that transduces environmental information to effect real-time control of holin function and thus of the length and fecundity of the phage infection cycle (21). However, despite these conceptual and mechanistic advances with T and RI, the genetic basis of the LIN phenomenon remains incomplete, some decades after the genetics of the *r* genes were first published, because no role has been found for *rIII* (1, 3). Although it was reported that RIII was not required for LIN on some K-12 strains (6), *rIII* shares with *rI* the features that neither locus can suppress *t* lysis-null mutations and both loci are transcribed from both early and late promoters (11, 27). Recently, *rIII* was suggested to play a role in the propagation of T4 in slow-growing host cells (28). Here we present the preliminary results of *in vivo* and *in vitro* characterization of *rIII*. The results are analyzed in terms of a model that suggests the direct molecular involvement of RIII in LIN as a new class of antiholin.

MATERIALS AND METHODS

Bacterial growth and induction. Table 1 provides a full list of phages and bacterial strains used in this study. Bacterial strains were plated on a standard LB agar plate supplemented with the appropriate antibiotics (ampicillin, 100 μg ml^{-1}; chloramphenicol, 10 μg ml^{-1}; kanamycin, 40 μg ml^{-1}). A single colony from an LB plate was used to inoculate a 3-ml overnight culture at 30°C for λ lysogens and at 37°C for nonlysogenic *Escherichia coli* strains, as described previously (21). Overnight cultures were diluted to an A_{550} of ~0.03 and were grown at 30°C or 37°C with aeration. Bacterial growth and lysis were monitored as described previously (21) using a Gilford Stasar III sipping spectrophotometer (Gilford Instrument Inc., Oberlin, OH). The λ lysogens were induced as described previously (14, 21). All plasmid-cloned genes were induced with 1 mM isopropyl-β-D-thiogalactopyranoside (IPTG).

Phage infection and preparation of phage lysates. Phage lysates were prepared by adding 10% $CHCl_3$ (vol/vol) to the *E. coli* cell culture after lysis, either in induced lysogens or by liquid culture infections, as described previously (19). The lysate was cleared by centrifugation at 5,000 × *g*, and the supernatant was filtered through a 0.22-μm syringe filter. Phage infection experiments were carried out as described previously (19, 21). For liquid culture infections, host *E. coli* cells were grown to an A_{550} of ~0.3 and were infected at a multiplicity of infection (MOI) of ~5. For the observation of plaque morphology, 100-μl overnight cultures of host cells were added to 3 ml of LB top agar, and the mixture was immediately poured onto standard LB agar plates. Five microliters of phage lysates with proper dilutions was spotted onto the top agar. For the complementation experiment, BL21(DE3) *fhuA*::Tn*10* cells carrying pET11a vectors were grown to an A_{550} of ~1 at 37°C and were induced with 1 mM IPTG for 2 h before being mixed with LB top agar and poured onto LB plates containing proper antibiotics and 1 mM IPTG. All plates were incubated for ~16 h at 37°C. The plaque sizes were analyzed using ImageJ software (NIH, Bethesda, MD).

Standard DNA manipulations and sequencing. All plasmids used in this study are listed in Table 1. Isolation of plasmid DNA, DNA amplification by PCR, DNA transformation, and DNA sequencing were performed as described previously (15, 22, 29). The DNA sequences of oligonucleotides (primers) are listed in Table 2. All purified oligonucleotides (primers) were purchased from Integrated DNA Technologies (Coralville, IA). Restriction and DNA-modifying enzymes were purchased from New England BioLabs (Ipswich, MA). The manufacturer's instructions for performing reactions were followed. The DNA sequences of all constructs were verified by a sequencing service provided by Eton Bioscience (San Diego, CA).

PCR and plasmid construction. T4D phage lysate was used directly as the PCR template for cloning out T4 genes. *Pfu* DNA polymerase was used for all PCRs by following standard protocols provided by Promega (Madison, WI). Site-directed mutagenesis was performed as described previously (22). The *rIII* gene, either with its native ribosome binding site (GAG) or with a stronger ribosome binding site (AGGAG), was cloned into the medium-copy-number, IPTG-inducible vector pZE12 (30). Plasmid pZE12-$RIII_o$ and pZE12-$RIII_s$ were constructed by inserting T4 DNA from nucleotide (nt) 130738 to nt 131080 ($RIII_o$), or from nt 130785 to nt 131033 ($RIII_s$), into pZE12 between the KpnI and XbaI sites. Plasmid pET11aRIII has the same insertion as pZE12$RIII_s$ between its NdeI and BamHI sites. Plasmid pZE12RI-RIII was made by inserting a tandem clone of *rI* and *rIII* genes with their original ribosome binding site into plasmid pZE12. These plasmids were transformed into a CQ21λ-t lysogen, in which the λ holin gene *S* has been replaced by T4 gene *t* (14). In this system, T can be expressed from the λ-t prophage and RI and/or RIII can be expressed in *trans* from pZE12 plasmids by adding 1 mM IPTG after lysogenic induction. A λS_{A52G} lysogen was used as a control, since S_{A52G} confers a ~20-min lysis time, similar to that with the *t* gene (31). Plasmid pTB146 is a derivative of plasmid pET11a encoding an N-terminal His_6-Sumo tag (29, 32). Plasmids encoding His-Sumo-tagged versions of RIII and nT (the N-terminal domain of T)—pTB146-RIII and pTB146-nT—were constructed by inserting codons 2 to 81 of the *rIII* gene, or codons 2 to 34 of the *t* gene (nt 160218 to nt 160322 of the T4 genome), respectively, into the pTB146 plasmid between its SapI and XhoI sites.

Constructing a T4 *rIII* deletion mutant. T4Δ*rIII* was constructed by homologous recombination between pZE12-Δ*rIII* and T4D, as described previously for T4Δ*rI* (19). pZE12-Δ*rIII* was made by deleting the *rIII* gene from plasmid pZE12-*rIII*-flank, which contains T4 DNA from nt 130231

TABLE 1 Phages, strains, and plasmids used in this study

Phage, bacterial strain, or plasmid	Description[a]	Source or reference(s)
Phages		
T4wt	Bacteriophage T4D	Laboratory stock
T4*rIII*	T4*r67*; H42-to-R (CAU-to-CGU) mutation in *rIII* locus	Laboratory stock
T4Δ*rI*	Complete deletion of *rI* from nt 59204 to nt 59496 in T4D genome	19
T4Δ*rIII*	Complete deletion of *rIII* from nt 130779 to nt 131042 in T4D genome	This study
λ-t	λ with holin gene *S* replaced with T4 holin gene *t*	14
λS_{A52G}	λcI857 carrying Ala52Gly early-lysis allele of *S* holin gene	31
T4rBB9	W16-to-stop (UGG-to-UGA) mutation in *rIII* locus	Laboratory stock
T4rES35	H42-to-Q (CAU-to-CAA) mutation in *rIII* locus	Laboratory stock
T4rES40	K82-to-E (AAG-to-GAG) mutation in *rIII* locus	Laboratory stock
Bacterial strains		
CQ21	*E. coli* K-12 *ara leu lacI*^{q} *purE gal his argG rpsL xul mtl ilv*	Laboratory stock
CQ21 λ-t	CQ21 lysogen carrying λ-t prophage	14
CQ21 λS_{A52G}	CQ21 lysogen carrying λS_{A52G} prophage	This study
BL21(DE3) *fhuA*::Tn*10*	*E. coli* B *ompT* r_B^- m_B^- (*P*$_{lac}$*UV5*::T7 gene 1) *slyD*::*kan fhuA*::Tn*10*	Laboratory stock
B834	*E. coli* B *ompT* r_B^- m_B^- *met*	Laboratory stock
MG1655	*E. coli* F^- λ^- *ilvG rfb-50 rph-1*	Laboratory stock
MDS12 *tonA*::Tn*10 lacI*^{q1}	MG1655 with 12 deletions, totaling 376,180 nt including cryptic prophages	19
DHP1	*E. coli* F^- *cya-99 araD139 galE15 galK16 rpsL1* (Str^r) *hsdR2 mcrA1 mcrB1*	36
Plasmids		
pZE12	ColE1 origin; $P_{LlacO-1}$ (PL promoter with three *lacO* operators); Amp^r	30
pZE12-luc	Luciferase gene *luc* cloned under the control of $P_{LlacO-1}$	30
pZE12RI	T4 *rI* cloned under the control of $P_{LlacO-1}$ with native SD	21
pZE12RIII$_o$	T4 *rIII* cloned under the control of $P_{LlacO-1}$ with native SD	21
pZE12RIII$_s$	T4 *rIII* cloned under the control of $P_{LlacO-1}$ with plasmid SD	This study
pZE12RI-RIII	Tandem clone of *rI–rIII* inserted between KpnI and XbaI sites	This study
pET11a-RIII	pBR322 origin, T7 promoter, carrying codons 1–82 of *rIII*	This study
pET11a-RIII$_{H42R}$	H42-to-R (CAU-to-CGU) mutation in *rIII*	This study
pTB146	*bla lacI*^{q} P_{T7}::*h-sumo*	32
pTB146-RIII	Codons 2–82 of *rIII* gene inserted between SapI and XhoI sites	This study
pTB146-nT	Codons 2–34 of *t* gene inserted between SapI and XhoI sites	This study
pCH364	T18-empty (Amp^r); N-terminal tag	36
pKNT25	Empty-T25 (Kan^r); C-terminal tag	35, 36
pKT25	T25-empty (Kan^r); N-terminal tag	35, 36
pCH364RIII	Codons 2–82 of *rIII* gene inserted between BamHI and EcoRI sites	This study
pKNT25RIII	Codons 2–82 of *rIII* gene inserted between XbaI and EcoRI sites	This study
pKT25nT	Codons 2–34 of *t* gene inserted between BamHI and EcoRI sites	This study

[a] SD, Shine-Dalgarno sequence.

to nt 131541 between its KpnI and XbaI sites, using our previously described method (33). Plasmid pZE12-Δ*rIII* was transformed into *E. coli* strain MDS12 *tonA*::Tn*10 lacI*^{q1}, and the transformants were grown to an A_{550} of ~0.4. The culture was infected with T4D phage at an MOI of 10 for 3 h at 37°C with aeration and was then lysed by adding 10% (vol/vol) $CHCl_3$. T4 *rIII* recombinants in this lysate were enriched three times for early lysis as described previously (19). The enriched lysate was plated onto *E. coli* B834 and was screened for *r* plaque morphology. The Δ*rIII* deletion was confirmed by PCR and sequencing.

SDS-PAGE and Western blotting. SDS-PAGE and Western blotting were conducted as described previously (22) Ten percent trichloroacetic acid (TCA) was used to precipitate proteins from the whole-cell samples. Reducing sample loading buffer (SLB) supplemented with β-mercaptoethanol was used for resuspending protein samples unless otherwise indi-

TABLE 2 List of oligonucleotides (primers) used in this study[a]

Primer name	Sequence
RIII$_S$ CLONING F	CGGTACATTAAACAATTACAACACGCTC
RIII$_S$ CLONING R	GGCTCTAGATTACTTCAGTGTTACCACAAAGTG
RIII$_S$ PET F	GGAATTCCATATGATTAAACAATTACAACACGCTC
RIII$_S$ PET R	GCGGGATCCTTACTTCAGTGTTACCACAAAGTG
RIII DEL +500 F	GGGGTACCCATCTGTTAACAAAAAGGAAAAACG
RIII DEL −500 R	GCTCTAGAGCGTTCAGATTAATCGTTTTCA
RIII DEL MIX F	TTTTAATCTCTAACGAGGGAGATTCACTGCCTTAGTGTGAGC
RIII DEL MIX R	CCGAGTTTTAATCTCTAACGAGGGAGATTCACTGCCTTAGT

[a] All oligonucleotides used were designed for this study.

cated. RIII proteins transferred to polyvinylidene difluoride (PVDF) membranes were detected using a rabbit polyclonal anti-RIII antibody purchased from GenScript (Piscataway, NJ). The monoclonal anti-His tag antibody was purchased from Sigma-Aldrich (Carlsbad, CA). To detect proteins, blots were incubated overnight at 4°C with anti-RIII or anti-His at a dilution of 1:4,000 in 3% milk–Tris-buffered saline (TBS) buffer. Blots were developed with the SuperSignal West Femto chemiluminescence kit, purchased from Thermo Fisher Scientific (Rockford, IL). The chemiluminescence signal was detected using a Bio-Rad ChemiDoc XRS system (Bio-Rad Laboratories, Hercules, CA). Images were obtained and analyzed by Quantity One 1-dimensional (1-D) analysis software (Bio-Rad Laboratories, Philadelphia, PA).

B2H assay. Bacterial two-hybrid (B2H) assays were conducted as described previously (34–36). Plasmids were constructed by inserting codons 2 to 81 of the *rIII* gene, or codons 2 to 34 of the *t* gene, into plasmids pCH363, pKNT25, pCH364, and pKT25, as described previously (36). Different pairs of plasmids were transformed into strain DHP1 and were grown to an A_{550} of ~0.3 in LB with 0.2% glucose and appropriate antibiotics (ampicillin, 50 μg ml^{-1}; kanamycin, 25 μg ml^{-1}). For the plate assay, 5 μl of cell cultures was spotted onto M9 minimal medium plates supplemented with 0.2% glucose, 40 μg ml^{-1} 5-bromo-4-chloro-3-indolyl-β-D-galactopyranoside (X-Gal), 150 μM IPTG, and proper antibiotics and was incubated for 48 h at 25°C.

Pulldown assays. Plasmid pET11a and pTB146 derivatives, described above, were transformed into BL21(DE3) *fhuA*::Tn*10* strains. Pulldown assays were conducted according to the instructions in the manufacturer's protocol from the Dynabeads His-Tag Isolation and Pulldown kit (Thermo Fisher Scientific, Rockford, IL). All incubations and reactions were carried out at 4°C, and beads were collected using a DynaMag-2 magnet (Thermo Fisher Scientific). All samples were resuspended in SLB and were boiled for 5 min to elute proteins, which were then analyzed by SDS-PAGE and Western blotting, performed as described above.

RESULTS

***rIII* is required for LIN in both *E. coli* B and *E. coli* K-12 backgrounds.** The role of *rIII* in LIN has been ambiguous, with reports differing as to whether *rIII* is required on *E. coli* B but not K-12 strains (6, 9, 37). In our hands, the classic *rIII* allele T4*r67*, which was used as the standard allele in the early T4 genetic map studies, formed r-type plaques on the lawns of both *E. coli* B834 and MG1655 (Fig. 2A); the plaques were somewhat smaller than those formed by T4*rI* but significantly larger than wild-type (wt) T4 plaques (Table 3). It was also reported that different T4 *rIII* mutants differed in plaque size, suggesting a possible correlation between the location of mutations on the *rIII* locus and plaque morphology (38). However, when we compared the plaque morphologies of four different T4 *rIII*-defective mutants (T4*rIII*, T4*rBB9*, T4*rES35*, and T4*rES40*) on B834, we did not observe significant differences (Table 3). Nevertheless, as the first step for interrogating the role of *rIII* in LIN, we constructed an *rIII* deletion allele, T4Δ*rIII*, to eliminate the potential for partial reversion. As shown in Table 3 and Fig. 2A, T4Δ*rIII* formed r-type plaques that were larger than wt plaques but smaller than those of T4Δ*rI*. Moreover, the wt plaque morphology could be complemented by a plasmid-borne *rIII* gene (Fig. 2B). In infections of both *E. coli* B and *E. coli* K-12 cultures under conditions where the wt T4 exhibited LIN, T4Δ*rIII* infections showed lysis at ~25 min, reproducibly later than the lysis time of T4Δ*rI* (~18 min), (Fig. 3A). The simplest notion, based on the established role of RI in LIN, is that RI expressed in the T4Δ*rIII* infection causes transient LIN and that, by extension, RIII is required for stable LIN in both *E. coli* B and K-12 strains.

Identification of the RIII protein. *rIII* encodes an 82-aa polypeptide without any secretion signals (Fig. 4A) and had not been identified as a protein species in T4-infected cultures. We raised a polyclonal antibody against an RIII oligopeptide sequence predicted to be highly immunogenic (Fig. 4A). The RIII protein could be visualized by immunoblotting in samples taken from cells infected with wt T4 but not with T4Δ*rIII* (Fig. 4B); the mobility of this RIII species corresponded to a molecular mass slightly lower than that predicted (8.9 kDa versus 9.3 kDa predicted), presumably due to the high content of charged residues (24 out of 82) (Fig. 4A).

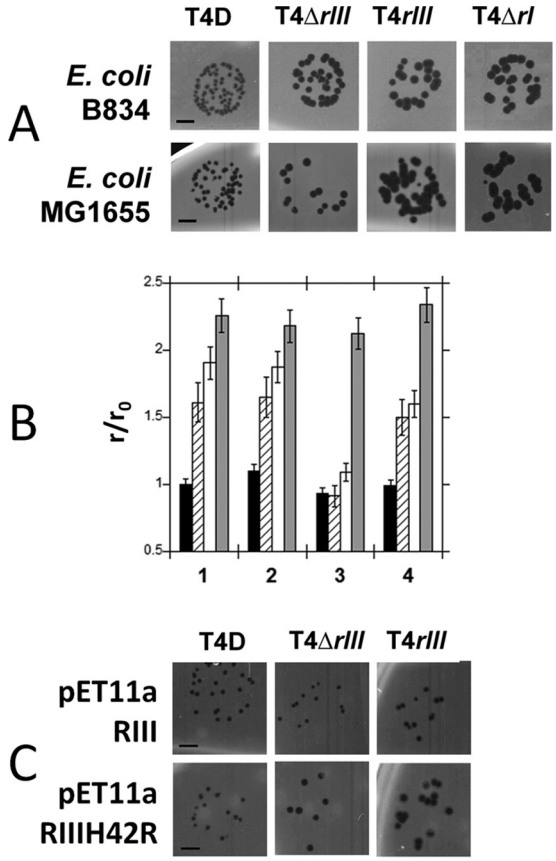

FIG 2 Plaque morphologies of T4 and its *r* mutants. (A) Plaque morphology of wt T4 (T4D) and T4 mutants on either an *E. coli* B strain (B834) or an *E. coli* K-12 strain (MG1655). Bars, 2.5 mm. The average plaque sizes of T4D, T4Δ*rIII*, T4*rIII*, and T4Δ*rI* on *E. coli* B834 or *E. coli* MG1655 are given in Table 3. (B and C) Complementation of *r* plaque morphology. (B) Differences in plaque sizes are shown as the ratio of the average phage plaque radius (r) to the average plaque radius of T4D plated on B834 (r_0). Black bars, T4D; hatched bars, T4Δ*rIII*; open bars, T4*rIII*; gray bars, T4Δ*rI*. Strains are indicated by numbers as follows: 1, MG1655; 2, BL21(DE3) *fhuA*::Tn*10* with no plasmid; 3, BL21(DE3) *fhuA*::Tn*10*/pET11a-RIII; 4, BL21(DE3) *fhuA*::Tn*10*/pET11a-$RIII_{H42R}$. (C) T4 *rIII* mutants plated onto *E. coli* strains expressing wt RIII restored wt T4 plaque morphology, whereas the expression of $RIII_{H42R}$ did not.

Recapitulating the role of RIII in LIN in the λ context. To address the role of RIII in LIN, we used a convenient system based on the inducible lambda prophage λ-t, in which the λ holin gene *S* is replaced by T4 *t* (14). Not only was this hybrid phage previously shown to recapitulate T4 lysis timing and LIN at physiological levels of expression; it allows the coexpression of selected T4 genes cloned in inducible plasmid vectors without the confounding ef-

TABLE 3 Mean diameters of phage plaques

Phage	Mean (±SD) diam (mm) of phage plaques in the following host:						
	B834	MG1655	BL21(DE3)	BL21(DE3)/pET11aRIII	BL21(DE3)/pET11aRIII-H42R	BL21(DE3)/pTB146	BL21(DE3)/pTB146-nT
T4D	0.57 (±0.04)	0.67 (±0.04)	0.63 (±0.06)	0.53 (±0.05)	0.57 (±0.05)	0.68 (±0.04)	1.07 (±0.05)
T4*rIII*	1.09 (±0.09)	1.43 (±0.07)	1.07 (±0.09)	0.62 (±0.03)	0.92 (±0.08)	1.32 (±0.08)	1.38 (±0.06)
T4Δ*rIII*	0.92 (±0.08)	1.12 (±0.06)	0.95 (±0.07)	0.52 (±0.06)	0.86 (±0.08)	1.13 (±0.08)	1.17 (±0.07)
T4Δ*rI*	1.29 (±0.09)	1.88 (±0.11)	1.24 (±0.07)	1.21 (±0.03)	1.34 (±0.06)		
T4*rBB9*	0.89 (±0.15)						
T4*rES35*	1.02 (±0.05)						
T4*rES40*	1.05 (±0.05)						

fects of T4-mediated host DNA degradation and translational repression (14, 15, 21, 39). This system mimics the T-dependent lysis in the λ context, where effects of T4 genes other than *t* are excluded. To provide RIII in *trans*, the *rIII* gene was cloned into the medium-copy-number plasmid vector pZE12 (30). Two isogenic clones were constructed with different Shine-Dalgarno (SD) sequences serving the *rIII* cistron: the relatively weak native sequence (GAG) and a stronger near-consensus sequence (AGGAG). The resulting plasmids, pZE12RIII$_o$ (where the subscript letter "o" indicates the original SD sequence) and pZE12RIII$_s$ (where the subscript letter "s" indicates the strong SD sequence), were transformed into the λ-t lysogen. Induction of the λ-t lysogen resulted in reproducible and sharply defined lysis at ~20 min; induction of pZE12RIII$_s$ with IPTG conferred a mild but reproducible lysis delay of ~5 min (Fig. 3B). In contrast, lysis was much more severely affected by the induction of an isogenic clone of the T4 antiholin gene *rI*, as shown previously (21). Induction of pZE12RIII$_o$ did not affect the timing of lysis, probably due to the lower protein expression level (data not shown).

We next asked if RIII can extend RI-mediated LIN. An isogenic plasmid with *rI* and *rIII* cloned in tandem was constructed and introduced into the λ-t lysogen. Induction of this plasmid, pZE12RI-RIII, led to drastically delayed LIN relative to that with induction of either pZE12RIII$_s$ or pZE12RI (Fig. 3B); under these conditions, the LIN state lasted as long as 80 min and then gradually deteriorated. Using this system, we tested three *rIII* missense alleles isolated by UV mutagenesis: the G24D, H42R, and A70V alleles (9) (Fig. 4A). In the absence of RI, two of the alleles, the G24D and H42R alleles, exhibited a slight but reproducible LIN defect, although the phenotype was subtle due to the relatively small effect of the parental *rIII* allele under these conditions (Fig. 3C, left). Coinduction of these *rIII* alleles with *rI*, however, resulted in distinct intermediate LIN defects, with lysis times ranging from 40 min to ~60 min, indicating that these are partially defective alleles, at least in the lambda context (Fig. 3C, right). The lysis blockage was *t* specific, as evidenced by the fact that isogenic experiments with a lambda holin allele, S_{A52G}, which has an early lysis phenotype that matches the normal *t* lysis time (31), did not show lysis delays in induction of pZE12RIII$_s$, pZE12RI, or pZE12RI-RIII (Fig. 3B). Taken together, these data indicated that RIII has T-specific antiholin activity.

RIII binds to the cytoplasmic N terminus of T. Next, we addressed the molecular basis of RIII participation in LIN. The simplest hypothesis is that, like other antiholins, including RI, RIII affects holin triggering by binding directly to holin T and blocking hole formation in the IM. Since RIII has no membrane or export signals (Fig. 4A), the only possible target for RIII is the N-terminal cytoplasmic domain of T (nT), which has 34 aa and is required for holin function (15). To test this idea, we used the bacterial two-hybrid system, based on intragenic complementation of CyaA function (34). We fused the nT, wt RIII, and four RIII mutant allele sequences to various combinations of T25 and T18 fragments of CyaA. As shown in Fig. 5A, this system revealed a strong self-interaction of RIII *in vivo*, which was abolished by the G24D allele, partially affected by H42R, and unaffected by L43Q or R75C. Transformants carrying plasmids expressing T18-RIII and T25-nT resulted in light but reproducible signals (Fig. 5B), suggesting a relatively weak interaction between RIII and nT. Significantly, none of the four RIII mutant fusion constructs retained nT-binding ability (Fig. 5B). These results correlate with the liquid culture lysis results (Fig. 3C) and indicate that the nT-RIII interaction is affected by the changes in the lysis-defective RIII alleles.

To address the nT-RIII interaction *in vitro*, we constructed versions of nT and RIII tagged at the N terminus with the His$_6$-Sumo moiety (see Materials and Methods). After induction in a T7-based overexpression system, both His$_6$-Sumo-nT and His$_6$-Sumo-RIII accumulated as soluble forms (Fig. 6, top, lanes 2 to 5). To detect complexes formed *in vitro*, the Sumo-tagged nT and RIII proteins were bound to magnetic beads, mixed with cell lysates containing wt RIII or mutant RIII$_{H42R}$ protein, fractionated (bound and unbound fractions), and then analyzed by immunoblotting. The results showed that both the wt RIII and mutant RIII$_{H42R}$ proteins form complexes with His$_6$-Sumo-RIII but that only wt RIII forms complexes with His$_6$-Sumo-nT (Fig. 6, bottom). The simplest interpretation is that the H42R mutation completely abrogates the RIII-nT interface but not the RIII homo-oligomerization interface, a pattern consistent with the results of the bacterial two-hybrid experiments.

The cytoplasmic N-terminal domain of T can block lysis inhibition in an RIII-specific manner. The finding that RIII binds nT *in vitro* and in *E. coli* in the context of the two hybrids suggested that the *r* phenotype could be imposed *in vivo* by titrating the RIII produced in a T4 infection with the Sumo-tagged nT derivative. To test this idea, we plated T4 onto lawns of cells in which His$_6$-Sumo-nT overexpression had been induced; under these conditions, wt T4 generated plaques distinctly larger and clearer than those generated on the isogenic control strain expressing the His$_6$-Sumo tag (Fig. 7). Neither T4*rIII* nor T4Δ*rIII* plaque morphology was affected by the overexpression of nT (Fig. 7).

DISCUSSION

Among the *Caudovirales*, the lysis timing effected by the holin defines the length and fecundity of the phage infection cycle. Mutational analysis has shown that holin-mediated lysis timing can be drastically altered by single missense changes (15, 39–41), leading to the suggestion that this extreme mutational

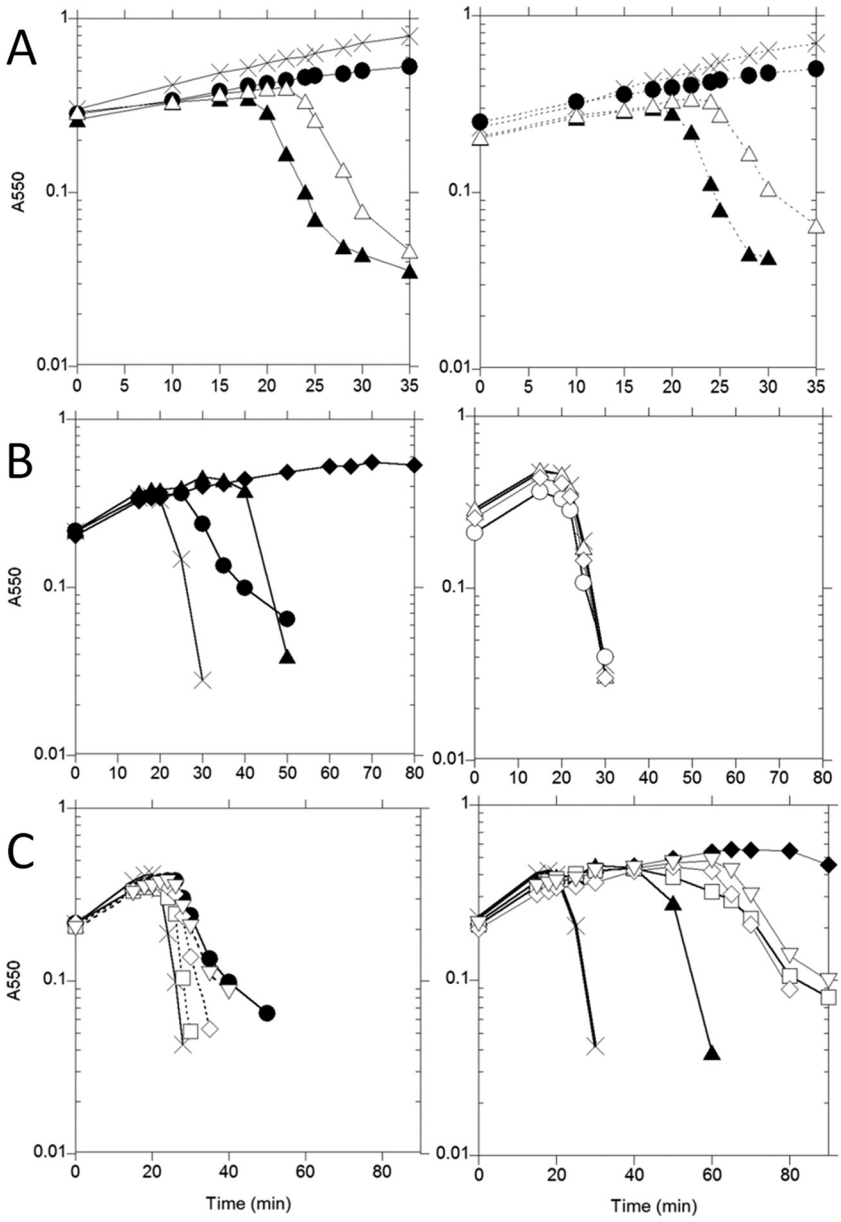

FIG 3 (A) Lysis in infections of *E. coli* B strain B834 (left) or *E. coli* K-12 strain MG1655 (right) with T4 and derivatives. ×, no phage; ●, T4D (wt); ▲, T4Δ*rI*; △, T4Δ*rIII*. Cultures were grown to an A_{550} of ~0.25 at 37°C and were then infected with T4 at an MOI of ~5. (B) Inductions (at time zero) of CQ21λ-t (left) or CQ21λS_{A52G} (right) lysogens carrying the indicated genes cloned under IPTG control in the context of the pZE12 plasmid. Plasmids were also induced by the addition of 1 mM IPTG at time zero. Multiplication signs, *luc* (negative control); triangles, RI; circles, $RIII_s$; diamonds, RI-RIII. (C) RIII missense mutants exhibit an intermediate LIN phenotype. CQ21λ-t lysogens carrying pZE12 plasmids with the indicated genes were induced at time zero. ×, *luc*; ▲, RI; ●, $RIII_s$; ◆, RI-RIII. (Left) □, $RIII_{G24D}$; ◇, $RIII_{H42R}$; ▽, $RIII_{A70V}$. (Right) □, RI-$RIII_{G24D}$; ◇, RI-$RIII_{H42R}$; ▽, RI-$RIII_{A70V}$.

sensitivity is an evolutionary fitness factor, allowing phages to mutate rapidly to a radically different life cycle length in response to altered environmental conditions (42). Despite the implied correlation between lysis timing and the environment, the T4 LIN phenomenon remains the only documented example of real-time regulation of lysis timing. Genetic analysis has shown that mutations in two of the classic T4 plaque morphology loci, *rI* and *rV*, the latter allelic to the *t* holin gene, confer an absolute defect in LIN. Our work had shown that RI is a secreted protein that is initially synthesized as a periplasmic protein tethered to the membrane with an N-terminal signal anchor release (SAR) domain (19). The presence of the SAR domain allows RI to be released into the periplasm and also confers extreme proteolytic instability on RI. Overexpression of the wt *rI* gene was shown to impose a delay on T-holin triggering in the lambda context (21). A chimeric *rI* gene in which the SAR domain was replaced by a cleavable signal sequence generated a proteolytically stable periplasmic RI and, expressed in *trans* with *t*, imposed a stable LIN state. A model has been proposed in which an unknown LIN signal is generated by a superinfecting T4 virion. Under these conditions, it is suggested that the T4 Spackle and Imm proteins force the su-

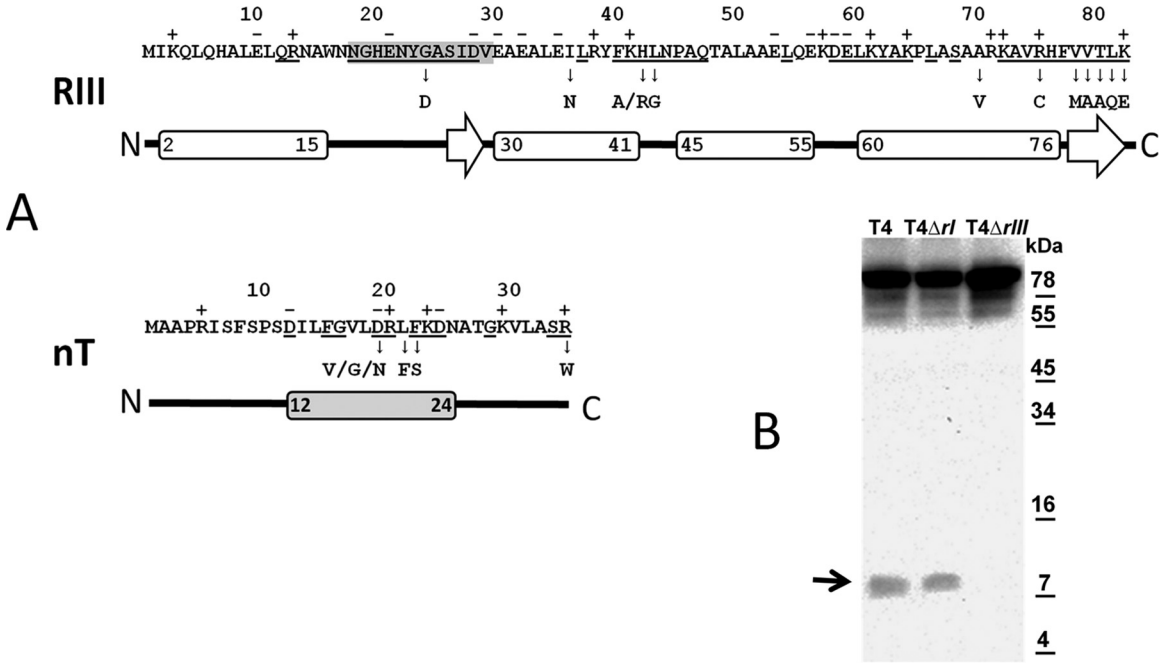

FIG 4 (A) Primary structure of RIII and the N terminus of T4 holin T (nT), with LIN-defective and lysis-defective alleles indicated by downward-pointing arrows. Conserved residues are underlined. The shaded area represents the oligopeptide used to raise the anti-RIII antibody. The predicted secondary structure is indicated as follows: open rectangles, helices; lines, turns; arrows, β-sheets; shaded rectangle, amphipathic helix. (B) RIII protein accumulates during infection. For each sample, 1 A_{600} equivalent of cells was loaded. The anti-RIII antibody was used in Western blotting. The arrow indicates the predicted molecular mass (9.3 kDa) for the RIII monomer.

perinfecting virion to eject its capsid contents ectopically into the host periplasm (43). Some component of these virion contents, which include both the T4 genomic DNA and ~1,000 protein molecules (11, 37), acts as a signal to stabilize the periplasmic RI protein. In this model, RI accumulates and binds to the periplasmic domain of the T4 holin T in such a manner that T triggering is inhibited (19). Significant progress has been made on the RI-T interaction. The soluble domain of RI, sRI, has been purified and shown to be largely α-helical in structure (22). In addition, the sRI molecule was able to bind the soluble domain of T, sT (22, 44) and prevent it from aggregating. Crystal structures of sRI and the sRI-sT complex have been determined (44). However, major gaps remained in our understanding of the LIN phenomenon. First, the signal provided by the superinfecting phage is completely unknown. In addition, the possible role of other *r* loci, most notably *rIII*, was not reflected in the model.

In this study, we have shown that *rIII*, as well as *rI*, is unambiguously required for LIN on both *E. coli* K-12 and B hosts, resolving a long-standing controversy (9, 11). Moreover, we have shown that the *rIII* gene, expressed in *trans* with the T4 holin gene *t*, can effect a small but reproducible lysis delay in a T-specific manner. In addition, *rIII* expression significantly stabilized the LIN state imposed by overexpression of wt *rI*, which otherwise imposes a lysis delay that collapses after ~45 min. Since RIII is a cytoplasmic protein, the simplest notion is that RIII acts by binding to the short cytoplasmic domain of T (nT). Evidence supporting this notion was obtained from bacterial two-hybrid analysis and pulldown assays, which revealed a specific interaction between nT and the full-length RIII poly-

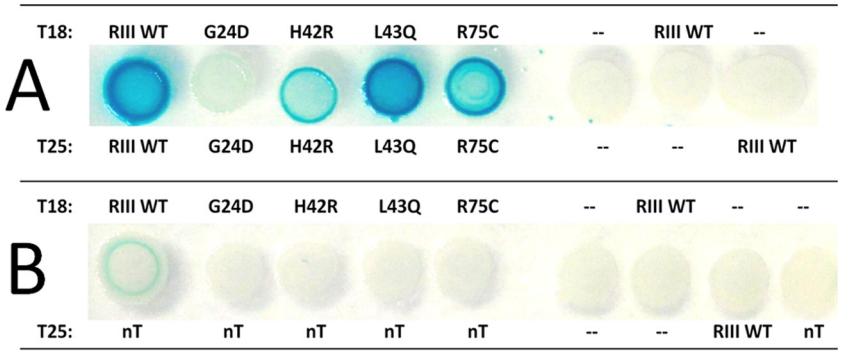

FIG 5 Bacterial two-hybrid results showing self-interaction of RIII (A) and interaction of RIII and the N terminus of T (nT) (B). T18, protein fused to the T18 fragment of CyaA protein; T25, protein fused to the T25 fragment of CyaA. T18 or T25 fragments without RIII or nT fusion serve as negative controls (−).

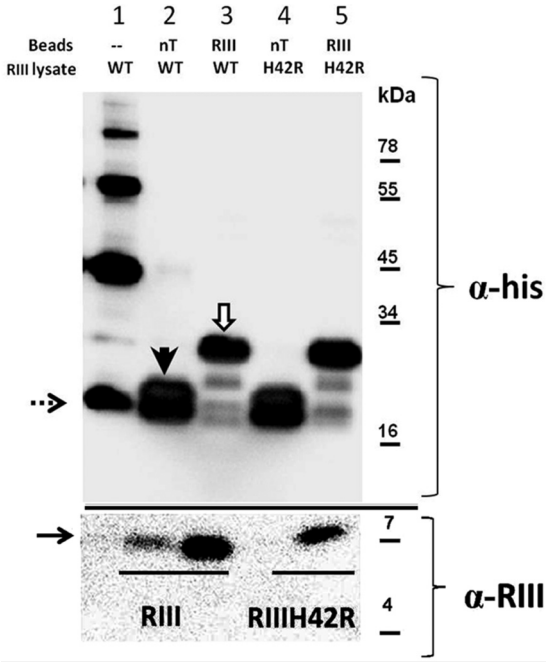

FIG 6 *In vitro* interaction between nT and RIII. His-Sumo-tagged nT or RIII was bound to anti-His Dynabeads, and RIII protein pulled down by Dynabeads was analyzed by Western blotting. (Top) Western blotting using an anti-His antibody. Lane 1, His-Sumo tag only (dashed arrow); lanes 2 and 4, His-Sumo-tagged nT (filled arrowhead), lanes 3 and 5, His-Sumo-tagged RIII (open arrow). (Bottom) RIII protein (arrow) is visualized by use of an anti-RIII antibody.

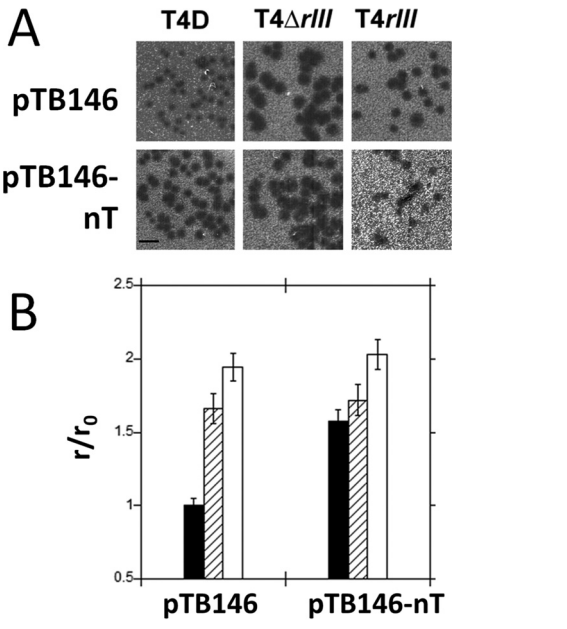

FIG 7 Rescue of *r* plaque morphology by overexpression of the N terminus of T (nT). (A) T4 phages were plated onto lawns of *E. coli* BL21(DE3) *fhuA*::Tn*10* carrying a control plasmid expressing His-Sumo-nT (pTB146-nT) or His-Sumo (pTB146; negative control). Bar, 2.5 mm. (B) The quantification of plaque sizes is shown as the ratio of the average plaque radius (r) to the average radius of T4D plaques plated on *E. coli* BL21(DE3) *fhuA*::Tn*10* (r_0). Filled bars, T4D; hatched bars, T4Δ*rIII*; open bars, T4r*III*.

peptide. Importantly, known dysfunctional *rIII* missense mutations caused a defect in the RIII-mediated stabilization of RI-LIN. Finally, bacterial two-hybrid evidence was provided showing that RIII has a dimerizing or oligomerizing propensity, which may be functionally important in view of the fact that one of the known *rIII*-defective missense mutations abrogates the response.

Taken together, these results indicate that both RI and RIII are, strictly defined, specific antiholins of the T4 holin T, and they suggest an expansion of our previous model to include inhibitory interactions on both sides of the cytoplasmic membrane (Fig. 8). In this scenario, RI acts as the LIN master regulator by receiving the signal generated by the superinfecting virion. Stabilization of RI leads to the formation of RI-T complexes that prevent the T protein from participating in the holin-triggering pathway. The available evidence indicates that holin triggering occurs when the holin reaches a critical 2-dimensional concentration and forms large oligomers, or rafts, within which the lethal holes are formed (42, 45). The simplest notion is that RI may simply block the homo-oligomerization, and thus the triggering, of T, a notion consistent with the ability of sRI to prevent the aggregation of sT (20). In our new model, we suggest that RIII participates in LIN by stabilizing the RI-T complexes. Indeed, the sRI-sT crystal structures were in the form of sT-sRI-sRI-sT heterotetramers (44). Thus, an attractive notion is that upon the onset of LIN, T-RI-RI-T heterotetramers are formed, providing a symmetric binding site at which RIII dimers can bind to the cytoplasmic nT domains (Fig. 8). It should be noted that, from this perspective, RIII is the first example of an antiholin with no secretory or membrane signal and also that the RI-RIII combination is the first example of a multiple-antiholin system.

As noted above, major gaps remain in our understanding of the T4 LIN phenomenon, which deserves attention not only because

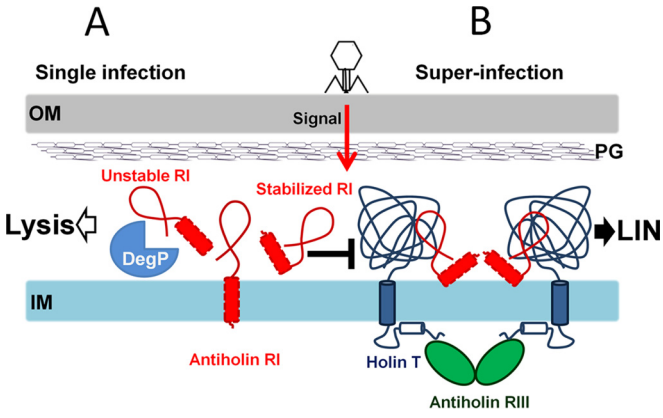

FIG 8 Current model of LIN involving two antiholins. Both RI and RIII are required for stable LIN. (A) In a single-phage infection, the antiholin RI will be degraded by the periplasmic protease DegP after spontaneous release into the periplasm. Cell lysis occurs at ~25 min. (B) In a superinfection, the DNA of a superinfecting T4 phage will be ectopically ejected into the periplasm, generating the "signal" to stabilize the periplasmic antiholin RI. This leads to the accumulation of RI, which then binds the periplasmic domain of T in a T-RI-RI-T heterotetramer. This facilitates the binding of the cytoplasmic antiholin RIII to the N terminus of T. This unique sandwich-like structure spanning two cell compartments robustly blocks the participation of T in hole formation.

of its historical status but also as a richly documented phenomenon that may be important for our understanding of phage propagation in liquid culture and of environmental scenarios that may be relevant to phage-based therapeutics. Immediate future efforts will be directed at determining the nature of the RIII-nT interaction at the structural level.

ACKNOWLEDGMENTS

This research was supported by Public Health Service grant GM27099 to R.Y. and by funding from the Center for Phage Technology (CPT). The CPT is jointly supported by Texas A&M University and Texas A&M AgriLife Research.

We thank Yi Duan and Allyssa Miller of the Herman laboratory for providing plasmids, strains, and advice for implementation of the bacterial two-hybrid assay. We also thank the Young laboratory and Center for Phage Technology members, past and present, for helpful discussions, criticisms, and suggestions.

FUNDING INFORMATION

This work, including the efforts of Ryland F. Young, was funded by HHS | U.S. Public Health Service (USPHS) (GM27099).

REFERENCES

1. **Hershey AD.** 1946. Mutation of bacteriophage with respect to type of plaque. Genetics **31:**620–640.
2. **Doermann AH.** 1948. Lysis and lysis inhibition with *Escherichia coli* bacteriophage. J Bacteriol **55:**257–276.
3. **Hershey AD, Chase M.** 1951. Genetic recombination and heterozygosis in bacteriophage. Cold Spring Harb Symp Quant Biol **16:**471–479. http://dx.doi.org/10.1101/SQB.1951.016.01.034.
4. **Benzer S.** 1955. Fine structure of a genetic region in bacteriophage. Proc Natl Acad Sci U S A **41:**344–354. http://dx.doi.org/10.1073/pnas.41.6.344.
5. **Crick FH, Barnett L, Brenner S, Watts-Tobin RJ.** 1961. General nature of the genetic code for proteins. Nature **192:**1227–1232. http://dx.doi.org/10.1038/1921227a0.
6. **Benzer S.** 1957. The elementary units of heredity, p 340–367. *In* McElroy WD, Glass B (ed), The chemical basis of heredity. Johns Hopkins University Press, Baltimore, MD.
7. **Hershey AD, Rotman R.** 1948. Linkage among genes controlling inhibition of lysis in a bacterial virus. Proc Natl Acad Sci U S A **34:**89–96. http://dx.doi.org/10.1073/pnas.34.3.89.
8. **Hershey AD.** 1946. Spontaneous mutations in bacterial viruses. Cold Spring Harb Symp Quant Biol **11:**67–77. http://dx.doi.org/10.1101/SQB.1946.011.01.010.
9. **Burch LH, Zhang L, Chao FG, Xu H, Drake JW.** 2011. The bacteriophage T4 rapid-lysis genes and their mutational proclivities. J Bacteriol **193:**3537–3545. http://dx.doi.org/10.1128/JB.00138-11.
10. **Krylov VN, Yankovsky NK.** 1975. Mutations in the new gene stIII of bacteriophage T4B suppressing the lysis defect of gene stII and gene *e* mutants. J Virol **15:**22–26.
11. **Paddison P, Abedon ST, Dressman HK, Gailbreath K, Tracy J, Mosser E, Neitzel J, Guttman B, Kutter E.** 1998. The roles of the bacteriophage T4 *r* genes in lysis inhibition and fine-structure genetics: a new perspective. Genetics **148:**1539–1550.
12. **Dressman HK, Drake JW.** 1999. Lysis and lysis inhibition in bacteriophage T4: *rV* mutations reside in the holin *t* gene. J Bacteriol **181:**4391–4396.
13. **Young R.** 1992. Bacteriophage lysis: mechanism and regulation. Microbiol Rev **56:**430–481.
14. **Ramanculov E, Young R.** 2001. Functional analysis of the phage T4 holin in a lambda context. Mol Genet Genomics **265:**345–353. http://dx.doi.org/10.1007/s004380000422.
15. **Moussa SH, Lawler JL, Young R.** 2014. Genetic dissection of T4 lysis. J Bacteriol **196:**2201–2209. http://dx.doi.org/10.1128/JB.01548-14.
16. **Josslin R.** 1970. The lysis mechanism of phage T4: mutants affecting lysis. Virology **40:**719–726. http://dx.doi.org/10.1016/0042-6822(70)90216-3.
17. **Summer EJ, Berry J, Tran TA, Niu L, Struck DK, Young R.** 2007. Rz/Rz1 lysis gene equivalents in phages of Gram-negative hosts. J Mol Biol **373:**1098–1112. http://dx.doi.org/10.1016/j.jmb.2007.08.045.
18. **Bode W.** 1967. Lysis inhibition in *Escherichia coli* infected with bacteriophage T4. J Virol **1:**948–955.
19. **Tran TA, Struck DK, Young R.** 2007. The T4 RI antiholin has an N-terminal signal anchor release domain that targets it for degradation by DegP. J Bacteriol **189:**7618–7625. http://dx.doi.org/10.1128/JB.00854-07.
20. **Tran TA, Struck DK, Young R.** 2005. Periplasmic domains define holin-antiholin interactions in T4 lysis inhibition. J Bacteriol **187:**6631–6640. http://dx.doi.org/10.1128/JB.187.19.6631-6640.2005.
21. **Ramanculov E, Young R.** 2001. An ancient player unmasked: T4 *rI* encodes a T-specific antiholin. Mol Microbiol **41:**575–583. http://dx.doi.org/10.1046/j.1365-2958.2001.02491.x.
22. **Moussa SH, Kuznetsov V, Tran TA, Sacchettini JC, Young R.** 2012. Protein determinants of phage T4 lysis inhibition. Protein Sci **21:**571–582. http://dx.doi.org/10.1002/pro.2042.
23. **Bläsi U, Chang CY, Zagotta MT, Nam KB, Young R.** 1990. The lethal lambda *S* gene encodes its own inhibitor. EMBO J **9:**981–989.
24. **White R, Tran TA, Dankenbring CA, Deaton J, Young R.** 2010. The N-terminal transmembrane domain of lambda S is required for holin but not antiholin function. J Bacteriol **192:**725–733. http://dx.doi.org/10.1128/JB.01263-09.
25. **To KH, Dewey J, Weaver J, Park T, Young R.** 2013. Functional analysis of a class I holin, P2 Y. J Bacteriol **195:**1346–1355. http://dx.doi.org/10.1128/JB.01986-12.
26. **Barenboim M, Chang CY, dib Hajj F, Young R.** 1999. Characterization of the dual start motif of a class II holin gene. Mol Microbiol **32:**715–727. http://dx.doi.org/10.1046/j.1365-2958.1999.01385.x.
27. **Luke K, Radek A, Liu X, Campbell J, Uzan M, Haselkorn R, Kogan Y.** 2002. Microarray analysis of gene expression during bacteriophage T4 infection. Virology **299:**182–191. http://dx.doi.org/10.1006/viro.2002.1409.
28. **Golec P, Karczewska-Golec J, Voigt B, Albrecht D, Schweder T, Hecker M, Wegrzyn G, Los M.** 2013. Proteomic profiles and kinetics of development of bacteriophage T4 and its *rI* and *rIII* mutants in slowly growing *Escherichia coli*. J Gen Virol **94:**896–905. http://dx.doi.org/10.1099/vir.0.048686-0.
29. **Berry J, Savva C, Holzenburg A, Young R.** 2010. The lambda spanin components Rz and Rz1 undergo tertiary and quaternary rearrangements upon complex formation. Protein Sci **19:**1967–1977. http://dx.doi.org/10.1002/pro.485.
30. **Lutz R, Bujard H.** 1997. Independent and tight regulation of transcriptional units in *Escherichia coli* via the LacR/O, the TetR/O and AraC/I_1-I_2 regulatory elements. Nucleic Acids Res **25:**1203–1210. http://dx.doi.org/10.1093/nar/25.6.1203.
31. **Johnson-Boaz R, Chang CY, Young R.** 1994. A dominant mutation in the bacteriophage lambda *S* gene causes premature lysis and an absolute defective plating phenotype. Mol Microbiol **13:**495–504. http://dx.doi.org/10.1111/j.1365-2958.1994.tb00444.x.
32. **Bendezú FO, Hale CA, Bernhardt TG, de Boer PA.** 2009. RodZ (YfgA) is required for proper assembly of the MreB actin cytoskeleton and cell shape in *E. coli*. EMBO J **28:**193–204. http://dx.doi.org/10.1038/emboj.2008.264.
33. **Hansson MD, Rzeznicka K, Rosenback M, Hansson M, Sirijovski N.** 2008. PCR-mediated deletion of plasmid DNA. Anal Biochem **375:**373–375. http://dx.doi.org/10.1016/j.ab.2007.12.005.
34. **Karimova G, Pidoux J, Ullmann A, Ladant D.** 1998. A bacterial two-hybrid system based on a reconstituted signal transduction pathway. Proc Natl Acad Sci U S A **95:**5752–5756. http://dx.doi.org/10.1073/pnas.95.10.5752.
35. **Battesti A, Bouveret E.** 2012. The bacterial two-hybrid system based on adenylate cyclase reconstitution in *Escherichia coli*. Methods **58:**325–334. http://dx.doi.org/10.1016/j.ymeth.2012.07.018.
36. **Miller AK, Brown EE, Mercado BT, Herman JK.** 2016. A DNA-binding protein defines the precise region of chromosome capture during *Bacillus* sporulation. Mol Microbiol **99:**111–122. http://dx.doi.org/10.1111/mmi.13217.
37. **Mathews CK, Kutter EM, Mosig G, Berget PB.** 1983. Bacteriophage T4. American Society for Microbiology, Washington, DC.
38. **Raudonikiene A, Nivinskas R.** 1992. Gene *rIII* is the nearest downstream neighbour of bacteriophage T4 gene 31. Gene **114:**85–90. http://dx.doi.org/10.1016/0378-1119(92)90711-W.
39. **Ramanculov E, Young R.** 2001. Genetic analysis of the T4 holin: timing and topology. Gene **265:**25–36. http://dx.doi.org/10.1016/S0378-1119(01)00365-1.
40. **Pang T, Park T, Young R.** 2010. Mutational analysis of the S21

pinholin. Mol Microbiol **76:**68–77. http://dx.doi.org/10.1111/j.1365-2958.2010.07080.x.
41. **Raab R, Neal G, Garrett J, Grimaila R, Fusselman R, Young R.** 1986. Mutational analysis of bacteriophage lambda lysis gene *S*. J Bacteriol **167:**1035–1042.
42. **Young R.** 2013. Phage lysis: do we have the hole story yet? Curr Opin Microbiol **16:**790–797. http://dx.doi.org/10.1016/j.mib.2013.08.008.
43. **Obringer JW.** 1988. The functions of the phage T4 immunity and spackle genes in genetic exclusion. Genet Res **52:**81–90. http://dx.doi.org/10.1017/S0016672300027440.
44. **Kuznetsov VB.** 2011. Structural studies of phage lysis proteins and their targets. Ph.D. dissertation. Texas A&M University, College Station, TX.
45. **To KH, Young R.** 2014. Probing the structure of the S105 hole. J Bacteriol **196:**3683–3689. http://dx.doi.org/10.1128/JB.01673-14.